Percolation in a simple cubic lattice with distortion

Sayantan Mitra, Dipa Saha, and Ankur Sensharma*
Department of Physics, University of Gour Banga, Malda - 732103, West Bengal, India

(Received 8 March 2022; accepted 22 August 2022; published 6 September 2022)

Site percolation in a distorted simple cubic lattice is characterized numerically employing the Newman-Ziff algorithm. Distortion is administered in the lattice by systematically and randomly dislocating its sites from their regular positions. The amount of distortion is tunable by a parameter called the distortion parameter. In this model, two occupied neighboring sites are considered connected only if the distance between them is less than a predefined value called the connection threshold. It is observed that the percolation threshold always increases with distortion if the connection threshold is equal to or greater than the lattice constant of the regular lattice. On the other hand, if the connection threshold is less than the lattice constant, the percolation threshold first decreases and then increases steadily as distortion is increased. It is shown that the variation of the percolation threshold can be well explained by the change in the fraction of occupied bonds with distortion. The values of the relevant critical exponents of the transition strongly indicate that percolation in regular and distorted simple cubic lattices belong to the same universality class. It is also demonstrated that this model is intrinsically distinct from the site-bond percolation model.

DOI: 10.1103/PhysRevE.106.034109

I. INTRODUCTION

Percolation is a fundamental model of statistical physics introduced in 1957 [1]. It is perhaps the simplest model to exhibit a nontrivial and rich critical behavior [2]. Its appealing features have been continuously attracting researchers since its inception. Not surprisingly, therefore, the research in percolation has flourished in exploring its potential applications in many fields [3–15]. At the same time, the model has given ample opportunities to theorists and mathematicians to address fundamental questions and resolve elusive challenges [16].

Two basic variants of this model are site percolation and bond percolation. In a classic site (bond) percolation problem, the sites (bonds) of a lattice can either be empty or occupied. Initially, a lattice with all empty sites (bonds) is considered, and the sites (bonds) are then occupied one by one with a probability p, called the occupation probability. If two neighboring sites (bonds) are occupied, they are said to be linked to each other. All these linked sites (bonds) form a cluster. For low p, many clusters of small size exist in the lattice. The clusters grow larger as p increases, and at a sufficiently high occupation probability, a giant cluster spans the lattice. For an infinitely large lattice, the spatial extent of the spanning cluster is also infinite. The first occurrence of such a cluster marks a phase transition, and the corresponding occupation probability is called the percolation threshold p_c. There is also another model called site-bond percolation [17,18], in which both the sites and bonds are considered together and occupied independently to achieve spanning. Apart from these basic models, there exist numerous other models in literature such as directed percolation [1,13], bootstrap percolation [19], explosive percolation [20,21], first passage percolation [22], and many more. The value of the percolation threshold depends on the type of the lattice (or network), as well as on the predefined rules of the process.

Physicists are generally more interested in characterizing phase transitions by determining relevant critical exponents. It is often observed that the different variants of percolation share almost the same values for the critical exponents, despite having very different percolation thresholds [23–26]. These models are then said to belong to the same universality class. Although these results indicate that the values of the exponents depend primarily on the dimension of the lattice, there are instances of nonuniversality, too, in two dimensions [27,28].

Natural systems are hardly perfectly ordered ones. Therefore studying the percolation properties of regular lattices leaves a gap between ideal and real situations. To incorporate natural irregularities, a new percolation model in a distorted square lattice was proposed [29]. In that model the sites of a regular lattice are systematically but randomly dislocated from their original positions in a regular lattice. The nearest-neighboring sites are connected only if their distance is less than a predefined value, called the connection threshold. It was found that spanning becomes difficult with distortion, and spanning is not possible even with 100% sites occupied if the connection threshold is less than the lattice constant of the regular lattice.

In this work we extend this model for a simple cubic lattice (SCL) with distortion. The simulations are performed with the Newman-Ziff algorithm [30,31], which is more powerful in characterizing the critical behavior of the percolation transition. It is observed that when the connection threshold is set equal to or greater than the lattice constant of the regular

*itsankur@gmail.com

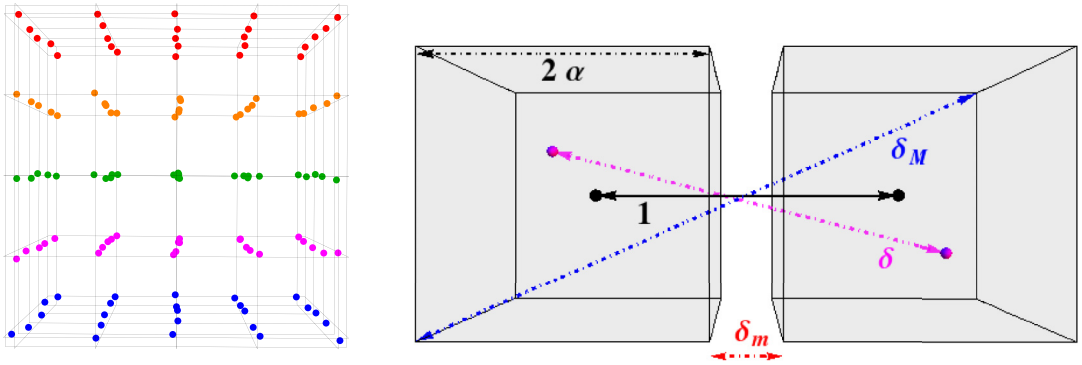

FIG. 1. (a) A realization of a 5×5 distorted SCL. This lattice has been constructed from a regular lattice of unit lattice constant by dislocating the sites following $\alpha = 0.05$. The viewing angle has been adjusted so that each row can be identified. (b) Magnified view of a pair of nearest neighbors in a distorted lattice. Each of them may be dislocated within a cube of length 2α centered at the regular lattice positions. The distance between these two centers is 1, while the distance between the sites is δ, which lies in the range $\delta_m \leqslant \delta \leqslant \delta_M$.

lattice, the percolation threshold of a distorted SCL increases with distortion. This behavior is similar to that of the distorted square lattice. However, when the connection threshold is less than the lattice constant, the percolation threshold first decreases and then increases with distortion. This is the most striking difference with the distorted square lattice, for which no spanning is possible if the connection threshold is less than the lattice constant. The similarity in the values of the critical exponents strongly suggests that the percolation in regular and distorted SCLs belong to the same universality class. We also demonstrate that percolation in distorted lattices cannot be thought of as another manifestation of site-bond percolation; these two models are distinct.

The paper is organized as follows: In Secs. II A and II B, we describe the method of generating the distorted SCL and the process of cluster building, respectively, in our model. Section III illustrates the central result of this paper—the impact of distortion on the percolation threshold p_c. In Sec. III A we calculate p_c of a finite lattice and show how it varies with the distortion parameter and the connection threshold. This is followed by the determination of an estimate of the percolation threshold of an infinite lattice p_c^∞ for some combinations of these two parameters (Sec. III B). Next we characterize the percolation transition by determining the critical exponents in Sec. IV and conclude that percolation in distorted and regular SCLs belong to the same universality class. Finally, in Sec. V we demonstrate that the present model is distinct from the site-bond percolation model before summarizing our findings.

II. THE MODEL

A. Generation of a distorted simple cubic lattice

In this model, site percolation is studied for a collection of sites arranged in a fashion that is nearly but not exactly an SCL. We call this a distorted simple cubic lattice. The lattice is distorted, because the positions of the sites are not in general on the regular lattice points but are slightly dislocated. Although the amount and direction of these dislocations are random and independent for each lattice point, control over the distortion has been enabled through the distortion parameter α. The process of generating such a lattice is explained below.

To begin with, a regular SCL of sites with lattice constant 1 is considered. A small cube of length 2α is considered around each site, keeping the site at the center of the cube. A given site is then dislocated to any position randomly within this small cube. This mechanism of shifting the positions of the sites is ensured by the following process. For each lattice point three separate random numbers, r_x, r_y, and r_z, each within the range $\{-\alpha, \alpha\}$, are generated for the shift of locations along x, y, and z directions, respectively. Each site is then shifted accordingly so that the regular lattice position (x, y, z) of a site changes to $(x + r_x, y + r_y, z + r_z)$. A distorted SCL is thereby realized. The amount of distortion can therefore be tuned by the parameter α.

Natural systems almost always have imperfections in their lattice structures. The idealized treatment of regular site percolation is therefore incomplete. The purpose of this study is to investigate the impact of these imperfections on percolation, and the focus is therefore at low to moderate distortion ($\alpha \leqslant 0.4$). Larger values of α would lead to almost a randomized array that falls outside the zone of interest of this work.

Figure 1(a) shows a schematic representation of a small distorted SCL. Note that the distance δ between a pair of nearest-neighbor sites is not a constant. As shown in Fig. 1(b), this distance may vary within the range $\delta_m \leqslant \delta \leqslant \delta_M$, where

$$\delta_m = 1 - 2\alpha, \tag{1}$$

and

$$\delta_M = \sqrt{1 + 4\alpha + 12\alpha^2}. \tag{2}$$

The variation of the nearest-neighbor distance δ is a key factor in the cluster building process, which is explained next.

B. Cluster building process

In usual percolation, if two neighboring sites of a regular SCL are occupied, they are automatically directly linked and are always considered to be in the same cluster. In contrast,

this is not guaranteed in a distorted SCL, since the distances between the nearest-neighbor pairs are not the same anymore. The connection criterion for two occupied neighbors is set by introducing a connection threshold d. A direct link between two occupied neighboring sites exists only if they are close enough to ensure $\delta \leqslant d$. Otherwise, the connection is broken even if both of them are occupied. Two limiting cases can readily be visualized from this criterion—if $d < \delta_m$, no cluster formation is possible, and if $d \geqslant \delta_M$, the usual site-percolation scenario is restored. Therefore the relevant ranges for δ and d are the same.

In this work, cluster numbering and identification have been done by the elegant Newman-Ziff (NZ) algorithm, which is known to give faster and more precise results as compared to other algorithms.

III. EFFECT OF DISTORTION ON THE PERCOLATION THRESHOLD

One of the major goals of this study is to observe how the percolation threshold p_c of an SCL is affected by distortion. It is anticipated that p_c should depend on the distortion parameter α as well as the connection threshold d. To determine $p_c(\alpha, d)$, a distorted lattice with a given α needs to be generated, and a connection threshold d needs to be set *a priori*. To demonstrate the variation of the percolation threshold with distortion, numerous combinations of α and d must be taken into account, and $p_c(\alpha, d)$ must be calculated for each of them.

All the existing rigorous and detailed methods to calculate a precise value for the percolation threshold p_c^∞ of an infinite lattice require a significant amount of computation time (see, for example, [26,32,33]). It is therefore impractical to go through one of these procedures to determine p_c^∞ for a large number of combinations of α and d. As a possible way out, we calculate p_c for a finite distorted SCL using the NZ algorithm. This enables us to show the variation of the percolation threshold in distorted SCLs with much less difficulty. Later, $p_c^\infty(\alpha, d)$ for some of the combinations of α and d have been calculated. It has been revealed that these values are satisfactorily close enough to the corresponding estimates. We reiterate that the goal of this study is not to calculate very precise percolation thresholds up to several decimal places but to understand the impact of α and d on p_c. This simple and quick estimation could therefore be very useful in gathering basic information of many other systems as well, before going for a detailed and rigorous method to obtain precise results for an infinite lattice.

A. Determination of $p_c(\alpha, d)$ for a finite lattice

First, a distorted SCL is generated with a fixed value of α. As explained earlier, the distances δ between the neighboring sites are not fixed anymore. A connection threshold d is then set to determine whether a given pair of occupied neighbors should be considered as directly connected (when $\delta \leqslant d$) or not (when $\delta > d$). Starting with an empty distorted SCL, the following sequence of steps is executed. These operations follow the basic structure of the NZ algorithm:

(1) Each site is marked with a specific number and its position is recorded.

(2) A randomized list is prepared to fix the order in which the sites are going to be occupied.

(3) The sites are then occupied one by one as per the prepared list.

(4) After occupying each site, the existence of links between occupied nearest neighbors is tested concerning the connection threshold d previously set. The cluster structure and root pointing are also examined and adjusted accordingly. (See Ref. [31] for the details of the NZ algorithm.)

(5) A checking is performed to detect the existence of a spanning cluster connecting two opposite sides of the lattice.

(6) If a spanning cluster is not found, the next site of the list is occupied and the last two steps are repeated.

(7) If a spanning cluster is found, no further sites are occupied and the occupation probability (the number of currently occupied sites divided by the total number of sites) is noted.

The above scheme is repeated for several independent realizations of the distorted SCL with the same α and keeping the same d for the connection criterion. The occupation probability p for which the spanning cluster first appears is recorded for each of the realizations. After averaging over all the recorded values of p, an estimated value of p_c is obtained for a fixed set of values of α and d. Since this method involves considerably less computation time, we could estimate p_c for nearly a thousand combinations of α and d. The calculations are done for distorted SCLs having $L = 2^7$ sites along each side. This means that the occupation probability changes by an amount $\Delta p = 1/L^3 = 4.77 \times 10^{-7}$ when a new site is occupied. The results are illustrated in Figs. 2(a) and 3. Every displayed point for p_c has been obtained by averaging over 1000 independent realizations of the distorted lattice with the same α and d.

Figure 2(a) shows 12 curves, one each for a fixed value of d, with α varying in the range $\{0, 0.3\}$, since we are interested in the low-to-moderate distortion regime. It is clear from the curves with $d > 1$ that distortion causes difficulty in spanning, and as a consequence the percolation threshold is increased. Although this feature is somewhat similar to that of the distorted square lattices, some crucial facts and distinctions should be mentioned here.

A very reliable estimate of the percolation threshold for a regular SCL is known to be $p_{cu} = 0.311\,607\,68(15)$ [26]. The curves with $d \geqslant 1$ start at this value (or, rather close to this value, as our calculation is for finite lattice) when $\alpha = 0$. This is expected—change in the connection threshold should not be manifested when distortion is absent. A glance at Eq. (2) reveals that $\delta_M = 1$ for $\alpha = 0$, and the condition $d \geqslant \delta_M$ to retain the regular percolation threshold is satisfied. This is also the reason why the curves for larger values of d stay at p_{cu} until α becomes large enough to ensure $d < \delta_M$.

A striking fact is noticed for $d = 1.0$ (i.e., the connection threshold is equal to the lattice constant): even a slight distortion makes a huge impact on the percolation threshold. The value of p_c stays close to p_{cu} when $\alpha = 0$, but it jumps to nearly twice of this value for a very small value of α. After this initial jump, however, p_c increases steadily with α.

We wish to remark here that no spanning cluster can be found for a distorted *square* lattice with $d \leqslant 1.0$, even when

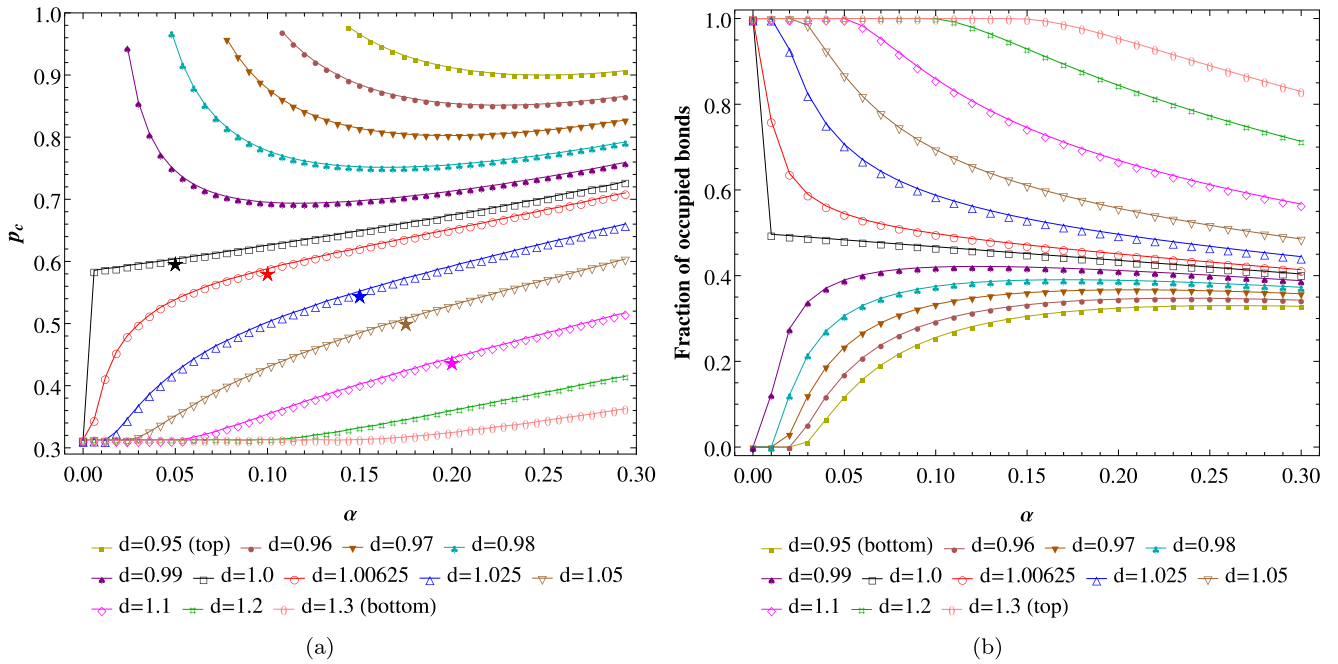

FIG. 2. (a) Variation of the percolation threshold p_c for a finite lattice with distortion parameter α. Each data point has been obtained by averaging over 10^3 realizations of a distorted SCL of $L = 2^7$. The curves are obtained simply by joining the points. Twelve curves are displayed for twelve different values of the connection threshold d. The five values of $p_c^{\infty}(\alpha, d)$ in Table I are indicated by stars. The natures of the curves are clearly different when $d \geqslant 1$ and $d < 1$. (b) Plots of fraction of occupied bonds with α show exactly the opposite nature for the same set of values of d. Each data point has been obtained by averaging over 10^3 realizations of a distorted SCL of $L = 2^7$. Occupancy of the bonds depends only on the construction of the lattice and is independent of the occupancy of the sites.

all the sites are occupied [29]. Although there exist some pair of occupied neighboring sites for which $\delta < 1$ (since $\delta_m = 1 - 2\alpha$), the fraction of occupied bonds can never become large enough to span a distorted square lattice. In contrast, for a distorted SCL, we do obtain spanning for $d < 1$ since a much lower fraction of occupied bonds (compared to a distorted square lattice) is required for spanning. In Fig. 2(a), five curves of $p_c(\alpha)$ are shown for $d = 0.99, 0.98, 0.97, 0.96$, and 0.95. These curves are of similar nature: an initial decline followed by a steady increment as α increases. This nature can be explained from Eq. (1), which says that the minimum distance δ_m between the nearest neighbors decreases with α. For extremely low values of α [$\alpha < (1 - d)/2$ in particular], $d < \delta_m$. Therefore no bonds are occupied. As α becomes bigger than this value, some of the bonds start to be occupied. At a certain value of α, the fraction of occupied bonds becomes sufficiently large enough to span the lattice, and we do obtain a finite value of p_c. When α is increased further, this fraction also increases [see Fig. 2(b)], which results in a decline in p_c. On the other hand, the average distance between the nearest neighbors slowly increases with α, since δ_M increases with α faster than δ_m decreases. This reduces bond occupancy. Therefore the decreasing trend cannot continue, and $p_c(\alpha)$ starts to increase steadily after forming a minimum. Note that no curves in Fig. 2(a) cross each other, and the curves for $d < 1$ always stay above the curves for $d \geqslant 1$.

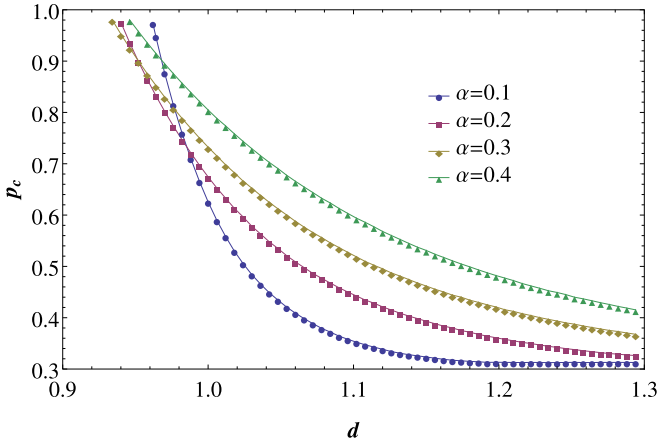

FIG. 3. The (approximate) percolation threshold p_c decreases with the connection threshold d. Each data point has been obtained by averaging over 10^3 realizations of a distorted SCL of $L = 2^7$. The curves are obtained simply by joining the points. Four curves are displayed for four different values of α. Spanning becomes easier as d increases, since more links are allowed.

As explained earlier, two neighboring sites are directly linked, or, in other words, the bond between them is "occupied" only if the distance between them is less than the connection threshold d. It should be noted that the occupancy of the bonds is fixed by the structure of the distorted lattice and is independent of whether the sites are occupied or not. Once a configuration is generated with fixed values of α and d, the number of occupied bonds gets fixed automatically. Thus a spanning path is formed through collaboration between the occupied sites and the occupied bonds. Consequently, when

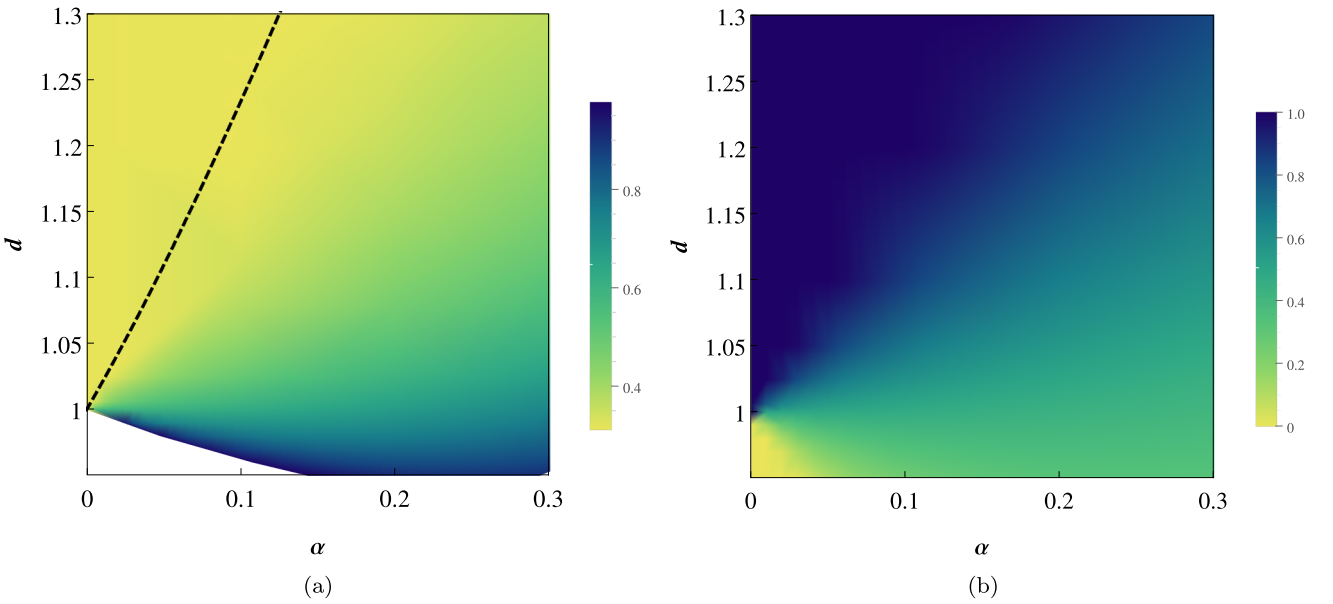

FIG. 4. (a) Variation of p_c with α and d. The magnitude of p_c is illustrated by color variation. The black dashed curve shows $\delta_M(\alpha)$ [Eq. (2)]. In the region on the left of this curve, $d > \delta_M$. Consequently, p_c remains constant at the value p_{cu} in this region. The colorless portion at the bottom-left corner indicates that no spanning cluster can be found in this range. (b) Variation of fraction of occupied bonds with α and d. The low-valued yellow patch at the bottom-left corner explains the absence of spanning cluster in this regime.

more bonds are occupied, the site percolation threshold p_c reduces. Therefore the variation of the percolation threshold with distortion has a direct correspondence with the variation of the fraction of occupied bonds. Figure 2(b) shows this dependence for the same set of values of d. It is clear that the nature of the curves for the corresponding values of d is exactly reversed. For $d \geqslant 1$, p_c always increases with α, while the fraction of occupied bonds always decreases. The jump for $d = 1$ is also present. When $d < 1$, p_c first decreases, forms a minimum, then increases steadily. Correspondingly, the fraction of bonds increases, forms a maximum, and then decreases steadily. Variation of p_c with the connection threshold d for different fixed values of α is shown in Fig. 3. Increase in d means more connections are allowed and consequently, existence of spanning cluster is more likely. It is therefore not surprising that p_c reduces with d. Here also p_c falls back to p_{cu} for low α and high d range when $d > \delta_M$ is satisfied (the curve for $\alpha = 0.1$). There exist some crossings between the curves in the $d < 1$ range. This can be anticipated by carefully observing the curves of Fig. 2(a). For example, it is clear that $p_c(\alpha = 0.1, d = 0.97) > p_c(\alpha = 0.2, d = 0.97)$, while $p_c(\alpha = 0.1, d = 1.1) < p_c(\alpha = 0.2, d = 1.1)$. Therefore a crossing between the $p_c(d)$ curves for $\alpha = 0.1$ and $\alpha = 0.2$ is inevitable.

Figure 4(a) shows the dependence of the percolation threshold on both α and d. The magnitude of p_c is represented by the color of the region—a darker shed means a higher value. As expected, p_c is high in the lower part of the figure where d is low. At the other extreme, p_c remains close to the value p_{cu}. The black dashed curve, showing δ_M as a function of α [see Eq. (2)], marks the boundary of this region. On the left of this curve $d > \delta_M$, so every connection between the nearest neighbors is allowed. When this happens, the percolation thresholds of the distorted and regular SCLs must be the same. The colorless portion at the bottom-left corner reveals the fact that no spanning cluster can be found in this range of values of α and d. The variation of the fraction of the occupied bonds is shown in Fig. 4(b). As expected, colors are reversed, since an increase in the number of bonds results in a lower percolation threshold. The yellow patch at the bottom-left corner means that the fraction of occupied bonds is small in this region. This explains why no spanning cluster is found for very small values of α when $d < 1$.

B. Estimation of $p_c^\infty(\alpha, d)$

The percolation threshold of an infinite lattice p_c^∞ marks the occupation probability p at which there is a sudden occurrence of an infinite cluster spanning the lattice. We calculate p_c^∞ through the information of the spanning probability $S(p)$—the probability of occurrence of a spanning cluster for a given occupation probability p. For finite lattices, the monotonically increasing curves of $S(p)$ become steeper as lattice size is increased, and finally, for an infinite lattice, the curve approaches the shape of a step function jumping from 0 to 1 at $p = p_c^\infty$. Therefore these curves of spanning probability for different lattice sizes should intersect each other at $p = p_c^\infty$.

To find p_c^∞ exploring the above concept, we generate $N = 10^5$ independent realizations of a lattice of size L with a fixed set of α and d. For each realization, some of the sites are occupied according to the occupation probability p. The number of realizations n_s having spanning cluster (with free boundary conditions) is counted. The fraction n_s/N approximately gives the spanning probability $S(p)$. In this way, the plots of $S(p)$ for lattice sizes $L = 32$, 48, 64, 96, and 128 have been generated. The obtained data points are interpolated to generate plots $S(p)$, and from the information of intersection points, p_c^∞ has been estimated. Figure 5 shows the plots of $S(p)$ for $\alpha = 0.2$ and $d = 1.1$, the step size of p being $\Delta p = 0.002$. Other

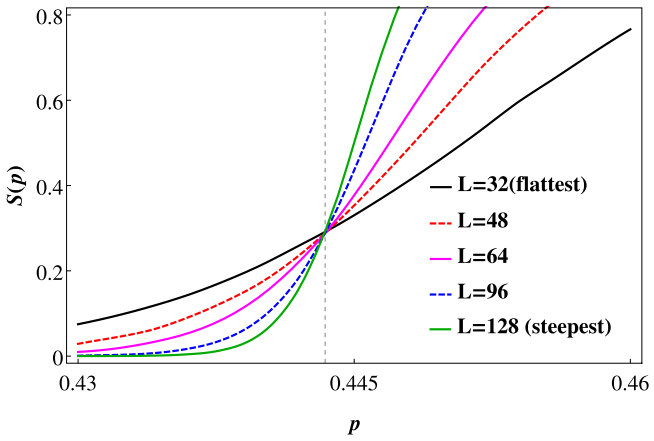

FIG. 5. Interpolated plots of spanning probability for five different sizes of distorted SCL with $\alpha = 0.2$ and $d = 1.1$. The obtained $p_c = 0.443\,42$ from all the intersection points is indicated by the vertical dashed line.

combinations are not shown, as they are similar in nature. It should be mentioned here that the accuracy is dependent on the sample size N, the number of lattice sizes considered, and the step size Δp.

Using the above method, p_c^∞ for a regular lattice has been found to be 0.311 562(18), which is satisfactorily close to the currently accepted values [32,33]. Table I shows $p_c^\infty(\alpha, d)$ for five combinations of α and d. These values are prominently indicated in Fig. 2(a). Note that in Fig. 2(a) the variation of p_c with α is shown, and separate curves are obtained for different values of d. While plotting the points of Table I, only the values of p_c^∞ and α have been provided.

IV. CRITICAL EXPONENTS AND UNIVERSALITY CLASS

Although the mechanism of connectivity in distorted lattices is not the same as the ordinary percolation, and the percolation threshold is also different, it is expected that the values of the critical exponents would remain the same as long as the modified mechanisms are short range. Nevertheless, it is worthwhile to verify this for the present model. Using the NZ algorithm, we focus on two important critical exponents β and ν, which are usually explored to decide on the universality class. Specifically, we determine the ratio β/ν and ν separately by two different methods. The obtained results indeed indicate that the values of these exponents do not depend on α and d. Also, these values are very close to those for ordinary percolation. Therefore we conclude that percolation in distorted SCLs belongs to the same universality class as standard percolation. The same conclusion has been reached for percolation in distorted square lattices [29,34]. It may therefore be stated that the distance-dependent spanning process of distorted lattices does not change the universality class.

A. Determination of ν

The critical exponent ν can be estimated by evaluating the wrapping probability $W(p)$, which is defined as the probability of finding a cluster that wraps around the lattice. Depending on the direction of wrapping, a few variants of $W(p)$ are usually calculated [30,31,33,35]. In this work, three such variants have been used for the estimation of ν. At a given occupation probability p, these three variants are defined as (i) $W_1(p)$: the probability that a cluster wraps around the lattice along a specified axis; (ii) $W_e(p)$: the probability that a cluster wraps around the lattice along any one axis; and (iii) $W_3(p)$: the probability that a cluster wraps around the lattice along all three axes. The exponent ν can be found out from these wrapping probabilities through the scaling relation

$$\left[\frac{dW(p)}{dp}\right]_{\max} \propto L^{1/\nu}. \tag{3}$$

To find any of the above wrapping probabilities $W(p)$ at a given occupation probability p, one can use the convolution

$$W(p) = \sum_{n=0}^{N} \binom{N}{n} p^n (1-p)^{N-n} \langle W(n) \rangle, \tag{4}$$

where $W(n)$ is the wrapping probability when n sites are occupied [31]. An advantage of this approach is that one can immediately find the first derivative without having to numerically differentiate. Differentiating Eq. (4),

$$\frac{dW(p)}{dp} = \sum_{n=0}^{N} \binom{N}{n} (n - Np) p^{n-1} (1-p)^{N-n-1} \langle W(n) \rangle. \tag{5}$$

We evaluate $W_1(n)$, $W_3(n)$, and $W_e(n)$ numerically using the NZ algorithm with periodic boundary conditions. Hence using Eqs. (4) and (5) we calculate the derivatives. The plots of dW_e/dp for system sizes $L = 16$, 24, 32, and 48 are shown for $\alpha = 0.2$ and $d = 1.1$ [Fig. 6(a)]. Plots of the other two wrapping probabilities look very similar. Locating $(dW/dp)_{\max}$ and taking logarithm of Eq. (3), ν can be evaluated from the gradient of the straight line [see Fig. 6(b)]. Obtained values of ν from the three types of wrapping probabilities for five

TABLE I. The values of the percolation threshold for infinite lattice and the critical exponents for five different combinations of α and d. Note that the critical exponents are essentially the same while the percolation threshold varies significantly.

α	d	p_c^∞	β/ν	d_f	ν from $[dW_3/dp]_{\max}$	ν from $[dW_1/dp]_{\max}$	ν from $[dW_e/dp]_{\max}$
0.05	1.0	0.60254(3)	0.468	2.532	0.889	0.883	0.883
0.1	1.00625	0.58688(4)	0.473	2.527	0.892	0.880	0.891
0.15	1.025	0.55075(2)	0.473	2.527	0.889	0.886	0.886
0.175	1.05	0.50645(5)	0.470	2.530	0.877	0.886	0.884
0.2	1.1	0.44342(3)	0.471	2.529	0.876	0.874	0.882

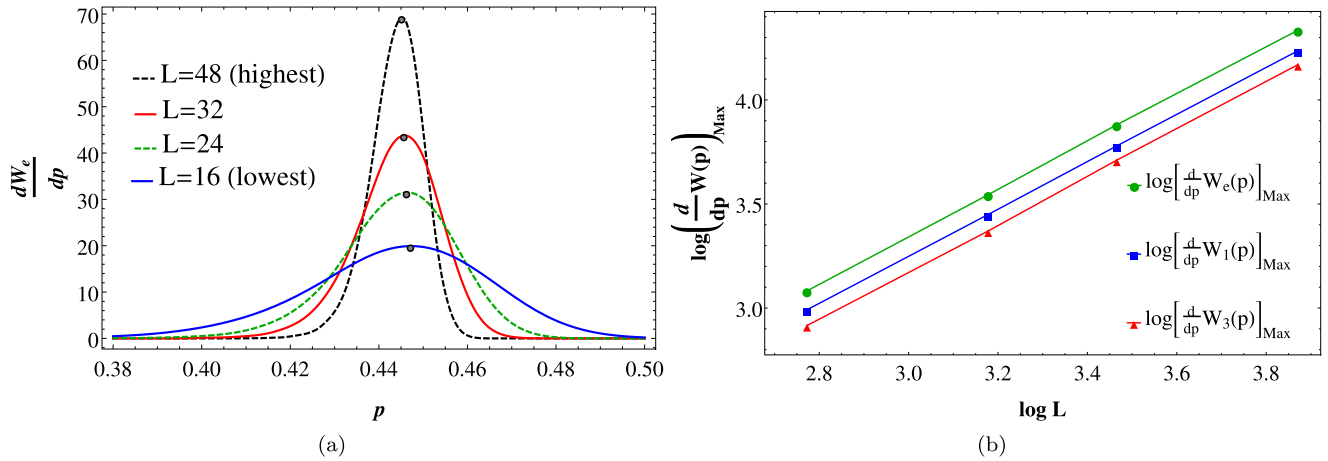

FIG. 6. (a) The plots of (dW_e/dP) for $L = 16, 24, 32, 48$. The maximum points used in the topmost line of (b) are shown by dots. (b) The log-log plot of $(dW/dP)_{\max}$ with L for the three wrapping probabilities W_1, W_e, and W_3. For all the plots of this figure, $\alpha = 0.2$ and $d = 1.1$.

combinations of α and d are summarized in Table I. These are close to the values found for a regular SCL [26,33,36]. The fluctuations are caused by the fact that $W_1(n)$, $W_3(n)$, and $W_e(n)$ are evaluated only over 10^3 configurations. However, even with this small sample size, the obtained values clearly suggest that ν has no dependence on α and d.

B. Determination of β/ν

The percolation order parameter is defined as

$$\Omega(L, p) = \frac{\langle S_{\max}\rangle}{L^{d_m}}, \tag{6}$$

where $S_{\max}$ is the size of the largest cluster at occupation probability p, L is the lattice size, and d_m is the dimension of the space. Here $\langle\rangle$ denotes the configurational average. It is known that $\langle S_{\max}\rangle$ is a fractal object at $p = p_c^\infty$ with fractal dimension d_f. Therefore,

$$\left\langle S_{\max}\left(p_c^\infty\right)\right\rangle \propto L^{d_f}. \tag{7}$$

The order parameter at the transition point is known to obey the scaling relation

$$\Omega\left(L, p_c^\infty\right) \propto L^{-\beta/\nu}. \tag{8}$$

Using Eqs. (6), (7), and (8) one can readily find

$$d_f = d_m - \beta/\nu. \tag{9}$$

With the information of p_c^∞ for five combinations of α and d, the ration β/ν is determined in the following manner. A distorted lattice of length L with a given combination of α and d is generated. To reduce the finite size effect, a periodic boundary condition needs to be enabled. $S_{\max}(p)$ is calculated for different occupation probabilities p. After averaging over 10^5 such lattices, $\langle S_{\max}\rangle$, and hence $\Omega(L, p)$ are determined. Variation of $\Omega(L, p)$ for $L = 16, 24, 32,$ and 48 are shown in Fig. 7(a) for $\alpha = 0.175$ and $d = 1.05$. The curves are obtained by connecting closely spaced data points. p_c^∞ for this combination has already been determined to be 0.506 45 and shown by the dashed vertical line. Points of the intersection of this line and the curves of $\Omega(L, p)$ give $\Omega(L, p_c^\infty)$. The plot of $\log \Omega(L, p_c^\infty)$ with $\log L$ should be a straight line with gradient β/ν [Eq. (8)]. In Fig. 7(b), five straight lines are shown for five $\{\alpha, d\}$ pairs of Table I. Each line is constructed by obtaining linear fit of four data points corresponding to $L = 16, 24, 32,$ and 48. β/ν can now be easily evaluated from the gradients of these lines. The lines of Fig. 7(b) are visibly parallel. It is not surprising, therefore, that the values of β/ν are very close to each other. Table I shows these five values. The values of d_f have been obtained from Eq. (9) using $d_m = 3$ for SCLs. These values are close to their corresponding values for a regular SCL [26,32,33,37].

It is known that the plots of $\Omega(L, p)$ of Fig. 7(a) should be collapsed when the horizontal and the vertical axes are scaled as $L^{1/\nu}(p - p_c)$ and $L^{\beta/\nu}\Omega(L, p)$, respectively. The exponent ν has been calculated in the previous section. Using $\beta/\nu = 0.47$, and one of the obtained values $\nu = 0.877$ for $\alpha = 0.175$ and $d = 1.05$ (see Table I), we indeed get a nice data collapse [see the inset of Fig. 7(a)].

The results of the critical exponents thus strongly indicate that the percolation in a regular and a distorted SCL belong to the same universality class.

V. DISTINCTION WITH SITE-BOND PERCOLATION

In site percolation, all the bonds are assumed to be preoccupied while a fraction of the sites is occupied as per occupation probability. Spanning occurs when a sufficient number of sites are occupied. The scenario is the opposite in the case of bond percolation, where all the sites are preoccupied and spanning is achieved by occupying bonds. There is another well-studied model called site-bond percolation, where neither all the sites nor all the bonds are preoccupied. Here, spanning is realized by randomly occupying a sufficient number of sites and bonds. Therefore occupation probability for sites and bonds need to be specified separately.

The present model appears to be somewhat similar to the site-bond percolation model. The only difference is that the occupation of the bonds in distorted lattices is conditional, while for site-bond percolation it is random. In a distorted lattice, the number of links connecting the nearest neighbors

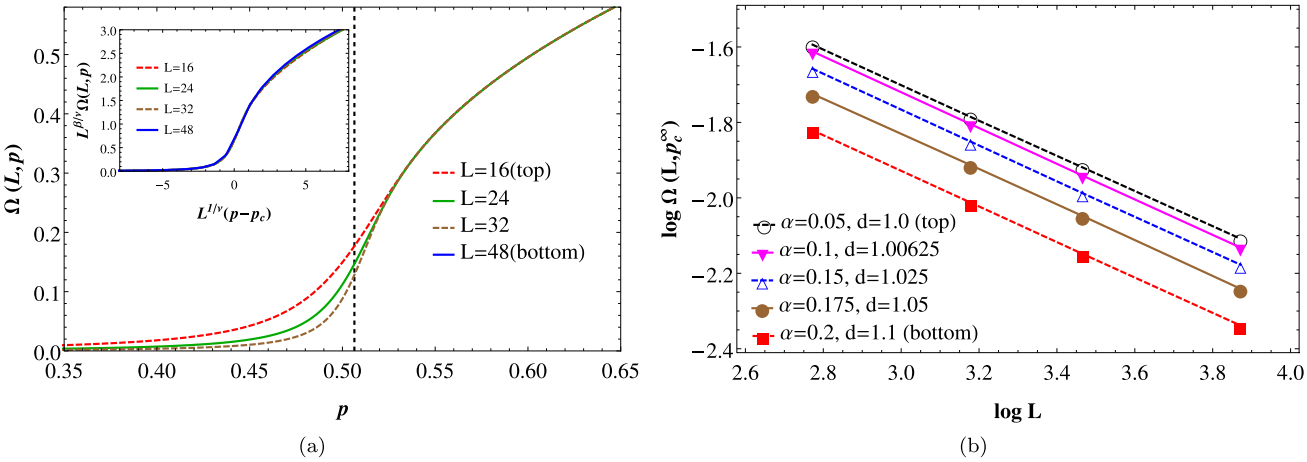

FIG. 7. (a) Plot of the order parameter $\Omega(L, p)$ for $L = 16$, 24, 32, and 48 with $\alpha = 0.175$ and $d = 1.05$. The corresponding p_c^∞ is indicated by the dashed vertical line. Inset: Data collapse using $p_c = 0.506\,45$, $\beta/\nu = 0.470$, and $\nu = 0.877$. (b) The log-log plot of the order parameter at percolation threshold $\Omega(L, p_c^\infty)$ with lattice size L. The five straight lines correspond to the five sets of values of α and d in Table I. The four points in each line correspond to $L = 16$, 24, 32, and 48. The lines are parallel since β/ν does not depend on α and d.

is fixed by the two parameters α and d. But in site-bond percolation, the fraction of the occupied bonds is specified by the bond occupation probability p_b. A natural question therefore arises: Are the site percolation thresholds of these two models the same when the same fraction of bonds are occupied (either randomly or conditionally)? If the answer is yes, one should conclude that the percolation in distorted lattices is just another manifestation of the site-bond percolation model. But we find that this is not the case. To establish this fact, we plot the site percolation thresholds for these two models with the fraction of the bonds (links) occupied (Fig. 8). As expected, the results of these two models coincide when all the bonds are occupied. However, for fewer occupied bonds, the site percolation thresholds (in Fig. 8 it is written as p_s) are clearly different for these two models. It should be understood

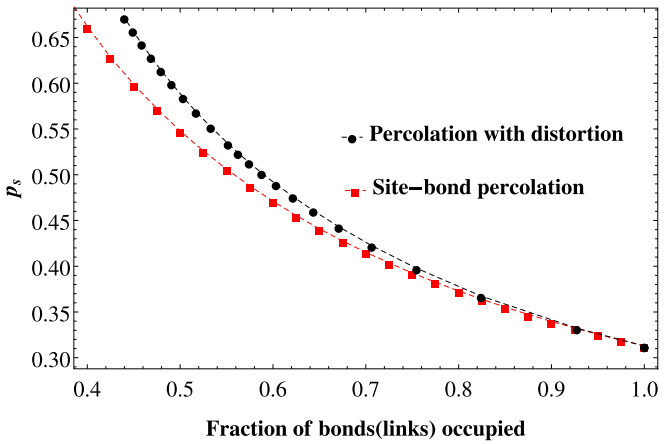

FIG. 8. Demonstration of distinction between site-bond percolation in regular SCL and site percolation in distorted SCL. The site percolation thresholds for these two models are not the same when same fraction of bonds is occupied. Each data point reflects an average over 10^3 realizations of a regular or distorted SCL with $L = 128$.

that, in a distorted lattice, the same fraction of links may be occupied for different combinations of α and d. We observe that p_s is the same for all of them. But when the same fraction of bonds is occupied for site-bond percolation, p_s is lower. So if a fraction f_0 of bonds or links are occupied, one may write

$$\left(p_s^{\text{distorted}}\right)_{f_0} \geqslant \left(p_s^{\text{site-bond}}\right)_{f_0}, \tag{10}$$

where the equality stands for $f_0 = 1$. To obtain the results of Fig. 8, the quick estimation method described in Sec. III A has been used for both models. The lattice size is $L = 128$, and each point is obtained after averaging over 10^3 configurations. The results of site-bond percolation are very close to those obtained by González *et al.* [38] through a more rigorous method. This confirms that percolation in distorted lattices is distinct from the site-bond percolation model.

VI. SUMMARY

To summarize, we have studied site percolation in distorted SCLs. A distorted SCL is prepared from a regular SCL (lattice constant = 1) by dislocating its sites randomly but systematically. The amount of distortion is tuned by the distortion parameter α. The distances between the neighboring sites of the distorted lattice are no longer the same, and two occupied neighboring sites are directly linked to each other if their distance is less than the connection threshold d. We develop a method to find the percolation threshold p_c for a finite lattice (plots are shown for $L = 2^7$) and later confirm that this estimate is satisfactorily close to the actual percolation threshold p_c^∞. The results are obtained by incorporating the distance-dependent connectivity of the neighboring sites into the Newman-Ziff algorithm. Our major findings are listed below.

(1) When the connection threshold d is fixed at a value $\geqslant 1$, the presence of distortion makes spanning difficult, as manifested by the increment in p_c with α. In particular, when

d is set to be equal to the lattice constant of the regular SCL, a discontinuous jump in p_c is noted for a very small distortion.

(2) However, for $d < 1$, p_c first decreases then increases steadily with α. This is a prominent difference with the results of a distorted square lattice, where no spanning cluster can be found for $d < 1$.

(3) On the other hand, p_c always decreases with d for a fixed value of α. Therefore the percolation threshold in distorted SCL depends heavily on the interplay between the two parameters α and d.

(4) To characterize the percolation transition, we calculate the critical exponents β, ν, and d_f, and find that they are very close to their currently accepted values for regular lattices. Although a considerable modification is enforced in the percolation process, and there is a significant change in the percolation threshold, the critical exponents remain essentially the same. Therefore we conclude that percolation in regular and distorted SCLs belong to the same universality class.

(5) Percolation in a distorted lattice appears to have some similarity with the site-bond percolation model. We have conclusively demonstrated that these two models are distinct from each other.

The goal of this study is to correctly characterize the percolation transition under the influence of distortion. Determination of the accurate percolation threshold and the critical exponents up to several decimal places is not aimed. We believe that the obtained results are sufficiently precise to reach the conclusions of this work.

The fact that distortion significantly impacts the percolation process has the potential to generate considerable scientific interest in the future. To proceed further with this model, distorted versions of other Bravais lattices may be investigated. It would also be interesting to see the effects of relaxing the number of nearest neighbors of a site and identifying them only in terms of their distances from the site. This scenario will be prominent in highly distorted 2D and 3D lattices, as well as in networks such as random geometric graphs. The works on percolation with extended neighborhood [39–41] may be useful in this regard.

ACKNOWLEDGMENTS

The authors thank Akhileswar Prasad and Bishnu Bhowmik for illuminating discussions. The computation facility at the Department of Physics, University of Gour Banga is gratefully acknowledged. D.S. acknowledges the ongoing fellowship (Ref. No. 1434/CSIR-UGC NET DEC. 2018) from the University Grants Commission of India.

[1] S. Broadbent and J. Hammersley, Percolation processes I. Crystals and mazes, Math. Proc. Cambridge Philos. Soc. **53**, 629 (1957).

[2] M. B. Isichenko, Percolation, statistical topography, and transport in random media, Rev. Mod. Phys. **64**, 961 (1992).

[3] Z. Ball, H. M. Phillips, D. L. Callahan, and R. Sauerbrey, Percolative Metal-Insulator Transition in Excimer Laser Irradiated Polyimide, Phys. Rev. Lett. **73**, 2099 (1994).

[4] V. S. Dotsenko, P. Windey, G. Harris, E. Marinari, E. Martinec, and M. Picco, Critical and Topological Properties of Cluster Boundaries in the 3D Ising Model, Phys. Rev. Lett. **71**, 811 (1993).

[5] I. A. Gruzberg, A. W. W. Ludwig, and N. Read, Exact Exponents for the Spin Quantum Hall Transition, Phys. Rev. Lett. **82**, 4524 (1999).

[6] I. Derényi, G. Palla, and T. Vicsek, Clique Percolation in Random Networks, Phys. Rev. Lett. **94**, 160202 (2005).

[7] A. Coniglio, H. E. Stanley, and W. Klein, Site-Bond Correlated-Percolation Problem: A Statistical Mechanical Model of Polymer Gelation, Phys. Rev. Lett. **42**, 518 (1979).

[8] S. G. Anekal, P. Bahukudumbi, and M. A. Bevan, Dynamic signature for the equilibrium percolation threshold of attractive colloidal fluids, Phys. Rev. E **73**, 020403(R) (2006).

[9] P. King, S. Buldyrev, N. Dokholyan, S. Havlin, Y. Lee, G. Paul, and H. Stanley, Applications of statistical physics to the oil industry: Predicting oil recovery using percolation theory, Physica A **274**, 60 (1999).

[10] B. Sapoval, A. Baldassarri, and A. Gabrielli, Self-Stabilized Fractality of Seacoasts through Damped Erosion, Phys. Rev. Lett. **93**, 098501 (2004).

[11] A. Ali Saberi, Percolation Description of the Global Topography of Earth and the Moon, Phys. Rev. Lett. **110**, 178501 (2013).

[12] E. V. Albano, Spreading analysis and finite-size scaling study of the critical behavior of a forest fire model with immune trees, Physica A **216**, 213 (1995).

[13] K. A. Takeuchi, M. Kuroda, H. Chaté, and M. Sano, Directed Percolation Criticality in Turbulent Liquid Crystals, Phys. Rev. Lett. **99**, 234503 (2007).

[14] P. Grassberger, On the critical behavior of the general epidemic process and dynamical percolation, Math. Biosci. **63**, 157 (1983).

[15] D. W. Zhou, D. D. Mowrey, P. Tang, and Y. Xu, Percolation Model of Sensory Transmission and Loss of Consciousness Under General Anesthesia, Phys. Rev. Lett. **115**, 108103 (2015).

[16] A. A. Saberi, Recent advances in percolation theory and its applications, Phys. Rep. **578**, 1 (2015).

[17] J.-P. Hovi and A. Aharony, Scaling and universality in the spanning probability for percolation, Phys. Rev. E **53**, 235 (1996).

[18] Y. Y. Tarasevich and S. C. Van der Marck, An investigation of site-bond percolation on many lattices, Int. J. Mod. Phys. C **10**, 1193 (1999).

[19] J. Adler, Bootstrap percolation, Physica A **171**, 453 (1991).

[20] D. Achlioptas, R. M. D'Souza, and J. Spencer, Explosive percolation in random networks, Science **323**, 1453 (2009).

[21] O. Riordan and L. Warnke, Explosive percolation is continuous, Science **333**, 322 (2011).

[22] J. M. Hammersley and D. J. A. Welsh, First-passage percolation, subadditive processes, stochastic networks, and generalized renewal theory, in *Bernoulli, Bayes, Laplace Anniversary*

Volume, edited by J. Neyman and L. M. LeCam (Springer-Verlag, New York, 1965), p. 61.

[23] C. D. Lorenz and R. M. Ziff, Precise determination of the bond percolation thresholds and finite-size scaling corrections for the sc, fcc, and bcc lattices, Phys. Rev. E **57**, 230 (1998).

[24] S. S. Manna and R. M. Ziff, Bond percolation between k separated points on a square lattice, Phys. Rev. E **101**, 062143 (2020).

[25] S. Kundu and S. S. Manna, Percolation model with an additional source of disorder, Phys. Rev. E **93**, 062133 (2016).

[26] X. Xu, J. Wang, J.-P. Lv, and Y. Deng, Simultaneous analysis of three-dimensional percolation models, Front. Phys. **9**, 113 (2014).

[27] M. K. Hassan and M. M. Rahman, Percolation on a multifractal scale-free planar stochastic lattice and its universality class, Phys. Rev. E **92**, 040101(R) (2015).

[28] S. Kundu and D. Mandal, Breaking universality in random sequential adsorption on a square lattice with long-range correlated defects, Phys. Rev. E **103**, 042134 (2021).

[29] S. Mitra, D. Saha, and A. Sensharma, Percolation in a distorted square lattice, Phys. Rev. E **99**, 012117 (2019).

[30] M. E. J. Newman and R. M. Ziff, Efficient Monte Carlo Algorithm and High-Precision Results for Percolation, Phys. Rev. Lett. **85**, 4104 (2000).

[31] M. E. J. Newman and R. M. Ziff, Fast Monte Carlo algorithm for site or bond percolation, Phys. Rev. E **64**, 016706 (2001).

[32] Y. Deng and H. W. J. Blöte, Monte Carlo study of the site-percolation model in two and three dimensions, Phys. Rev. E **72**, 016126 (2005).

[33] J. Wang, Z. Zhou, W. Zhang, T. M. Garoni, and Y. Deng, Bond and site percolation in three dimensions, Phys. Rev. E **87**, 052107 (2013).

[34] H. Jang and U. Yu, Universality class of the percolation in two-dimensional lattices with distortion, Physica A **527**, 121139 (2019).

[35] H. Yang, Alternative criterion for two-dimensional wrapping percolation, Phys. Rev. E **85**, 042106 (2012).

[36] M. Borinsky, J. A. Gracey, M. V. Kompaniets, and O. Schnetz, Five-loop renormalization of ϕ^3 theory with applications to the Lee-Yang edge singularity and percolation theory, Phys. Rev. D **103**, 116024 (2021).

[37] N. Jan and D. Stauffer, Random site percolation in three dimensions, Int. J. Mod. Phys. C **09**, 341 (1998).

[38] M. I. González, P. M. Centres, W. Lebrecht, and A. J. Ramirez-Pastor, Site-bond percolation on simple cubic lattices: Numerical simulation and analytical approach, J. Stat. Mech. (2016) 093210.

[39] Z. Xun, D. Hao, and R. M. Ziff, Site percolation on square and simple cubic lattices with extended neighborhoods and their continuum limit, Phys. Rev. E **103**, 022126 (2021).

[40] Z. Xun and R. M. Ziff, Bond percolation on simple cubic lattices with extended neighborhoods, Phys. Rev. E **102**, 012102 (2020).

[41] Z. Xun, D. Hao, and R. M. Ziff, Site and bond percolation thresholds on regular lattices with compact extended-range neighborhoods in two and three dimensions, Phys. Rev. E **105**, 024105 (2022).